

Molecular Interactions of Zinc Finger Protein Kaiso with Hemimethylated DNA

B. Thapa and N. P. Adhikari

Journal of Nepal Physical Society

Volume 9, Issue 1, June 2023

ISSN: 2392-473X (Print), 2738-9537 (Online)

Editor in Chief:

Dr. Hom Bahadur Baniya

Editorial Board Members:

Prof. Dr. Bhawani Datta Joshi

Dr. Sanju Shrestha

Dr. Niraj Dhital

Dr. Dinesh Acharya

Dr. Shashit Kumar Yadav

Dr. Rajesh Prakash Guragain

JNPS, 9 (1): 1-10 (2023)

DOI: <https://doi.org/10.3126/jnphysoc.v9i1.57551>

Published by:

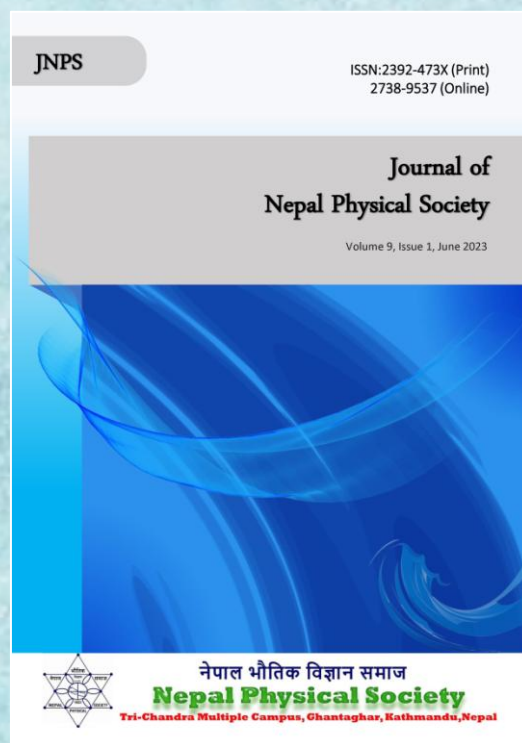
Nepal Physical Society

P.O. Box: 2934

Tri-Chandra Campus

Kathmandu, Nepal

Email: nps.editor@gmail.com





Molecular Interactions of Zinc Finger Protein Kaiso with Hemimethylated DNA

B. Thapa^{1,2} and N. P. Adhikari^{1,*}

¹Central Department of Physics, Tribhuvan University, Kirtipur, Kathmandu, Nepal

²Padma Kanya Multiple Campus, Tribhuvan University, Bagbazar, Kathmandu, Nepal

*Corresponding Email: narayan.adhikari@cdp.tu.edu.np

Received: 14th March, 2023; Revised: 24th May, 2023; Accepted: 17th June, 2023

ABSTRACT

DNA methylation is an epigenetic modification that is involved in various essential cellular processes. Methyl CpG binding proteins (MBPs), such as zinc finger protein Kaiso, bind with methylated DNA and mediate to translate methylation signal into the transcription process. To have mechanistic understanding of how these proteins recognize and interpret the DNA methylation signal is important because of their critical role in regulation of gene expression in both normal and diseased cells. In this study, we performed molecular dynamics (MD) simulation to investigate the recognition and binding of hemimethylated (methylation in one strand of double stranded DNA) sequences by Kaiso to assess the role of methylation in each strand. We investigated the major interactions involved in the complex formation as well as the contact area and binding free energy of the Kaiso-DNA complexes. Our results show that the number and strength of hydrogen bonds as well as other non-bonded interactions are greater in Kaiso-DNA complex with methylated CpG sites in non-coding strand. Similarly, the contact area at the Kaiso-DNA interface and binding free energy of Kaiso is also higher in hemimethylated sequence having methylation in non-coding strand. Therefore, methylated CpG sites in non-coding strand play important role in the binding of Kaiso with methylated DNA sequences.

Keywords: DNA methylation, Molecular Dynamics simulation, Hemimethylated DNA, Hydrogen bonds.

1. INTRODUCTION

DNA methylation is a crucial epigenetic mark, a stable and inheritable chemical change that alters gene expression without any change in DNA sequence [1]. This modification is resulted from the covalent addition of methyl group to the 5- carbon position of Cytosine (5mC) base of DNA [1, 2]. DNA methylation plays important role in many cellular mechanisms including gene expression regulation, genetic imprinting, X-chromosome inactivation, and cellular differentiation during embryogenesis, genetic stability maintenance [3, 4, 5, 6]. The aberrant methylation patterns are known to have major consequences in embryonic development and are associated with birth defect, autoimmune disease, and several neuro-developmental diseases [7, 8]. Moreover, alteration

in normal methylation levels are implicated in various cancers [8].

DNA methylation can regulate the gene expression mainly in two ways. First, DNA methylation affects the promoter regions of the gene and inhibits the binding of transcription factors proteins, thereby directly bringing about gene repression [9]. Secondly, specific families of proteins are attracted to methylated DNA sequences that mediate transcription repression indirectly. The transcription factors that are evolved to preferentially bind to methylated CpG (mCpG) sites are known as methyl-CpG-binding proteins (MBPs) [10, 11]. Upon binding to the methylated sites, they recruit co-repressor complexes and histone deacetylases, which subsequently remodel the chromatin structure into transcriptionally inactive state and

thereby inhibiting the gene expression [12]. Mainly, three classes of MBPs have been identified which selectively recognize methylated CpG sites. The methyl binding domain (MBD) proteins are initially identified MBPs, which recognize the symmetrically methylated CpG dinucleotides [13]. Another family of MBPs is “SET and RING finger-associated” (SRA) domain proteins, which bind specifically to hemimethylated DNA sequences [14]. The third family of MBPs is the zinc finger (ZF) proteins that recognize the two consecutive pair of symmetrically methylated CpG sites [15, 16, 17].

As the archetypal member of BTB/POZ subfamily of zinc finger proteins (POZ-ZF), Kaiso was first identified as the binding partner of p120 catenin protein in 1999 [18]. The three C2H2 ZF domains of Kaiso in C-terminal region are involved in DNA binding and the N-terminal BTB/POZ domain is involved in homo-dimerization as well as interaction with other proteins [18, 19, 20]. Kaiso specifically binds to the symmetrically methylated DNA with preference to the two consecutive methylated CpG dinucleotides (mCpG) in its recognition sequence [19]. In addition to methylated CpG sites, Kaiso also binds to the unmethylated consensus sequence also known as Kaiso binding site (KBS) [20]. Kaiso shows the bimodal activity for the transcription regulation, it both acts as transcription repressor as well as activator [21]. It is found to be over-expressed in several human cancers, such as colon, breast, and prostate [22, 23, 24]. Because of its direct involvement in different cancers, the mechanistic understanding of how Kaiso recognize the methylated DNA and mediate to translate the methylation signal into cellular outcome is important.

Previous studies [25, 26, 27, 28] have shed light on the recognition mechanism of two consecutive symmetrically methylated DNA sequences by Kaiso. Mainly, Kaiso binds with the methylated DNA (meDNA) sequences through the alpha helices in the ZF domains. The base-specific hydrogen bonding interactions with the DNA bases occur via the ZF1 and ZF2. Similarly, several other non-base-specific hydrogen bonding interaction with ZF3 and the C-terminal extension loop are involved in the binding and stability of the Kaiso-meDNA complexes [25, 27]. However, there is no molecular level investigation on the impact of methylation in each strand in the binding with Kaiso with meDNA. In this study, we have studied

the dynamics of the interaction of Kaiso with hemimethylated DNA sequences. More specifically, we have assessed the contribution of methylation in each strand on the recognition and stability of the complex. We have investigated the various non-covalent interactions such as hydrogen bonding, electrostatic and van der Waals interaction involved in the binding of Kaiso with hemimethylated DNA sequences. The interactions and the binding affinity of Kaiso with DNA is stronger in case of the methylation in non-coding strand (with 5mC26 and 5mC28) than in coding strand (with 5mC8 and 5mC10). Our results show that binding of Kaiso is significant in each strand; however, it prefers the methylation in the non-coding strand.

2. MATERIALS AND METHODS

2.1 Molecular structures and system setup

The molecular structures for the Kaiso protein and DNA sequences were taken from the Protein Data Bank. We modeled MeECad_mod complex, taking the DNA sequence from MeECad complex (with PDB ID 4F6N) and protein from MeCG2 complex (with PDB ID 5VMV) as in our previous work [27]. The nucleotide sequences in MeECad are of the form 5'-GTGTCACmCGmCGTCTATAG-3'; with two pairs of mCpG sites in both strands of DNA. In this work, we generated mutated complex (referred to as hemi_C) by mutating the methylated cytosines in the non-coding strands of MeECad (5mC26 & 5mC28) into cytosines (CYT26 & CYT28). Similarly, another mutant complex (referred to as hemi_NC) was generated by mutating the methylated cytosines in the coding strands of MeECad (5mC8 & 5mC10) into cytosines (CYT8 & CYT28). The N-terminal missing residues (471-480) and C-terminal missing residues (597-604) were modeled using Charmm-GUI web server [28]. The system preparation and inputs files for the simulation were also created using Charmm-GUI. To mimic the cellular environment, we have solvated both the Kaiso-DNA systems using TIP 3 water model in the cubical boxes with 10 Å padding around the complex and neutralized by adding NaCl with the concentration of 0.15 M. Total number of atoms in hemi_C and hemi_NC complexes are 49,083 and 49,071 respectively. The system size for both of the Kaiso-DNA complexes are $81 \times 81 \times 81 \text{ \AA}^3$.

2.2 Molecular Dynamics Simulations

All-atom MD simulations were performed with NAMD simulation package [29] using CHARMM36m force field [30]. MD simulation

was carried out following the standard method of energy minimization, equilibration and production runs. The energy minimization of the system was performed for 10,000 steps using the conjugate gradient and line search algorithm. The equilibration run was done at room temperature (300K) for 125 ps with 1 fs integration time step. During equilibration protein's heavy atoms in the backbone were harmonically restrained with a force constant of 1.0 kcal/mol/Å and side chain atoms were restrained with force constant of 0.1 kcal/mol/Å. Particle Mesh Ewald (PME) method [31] was employed to calculate the long-range interactions. The cut off distance of 12 Å taken for non-bonded interactions. The production runs were performed in NPT conditions at 300 K with fully unrestrained protein with a time step of 2 fs. The production runs for each system was carried out for 100 ns.

2.3 Data Analysis

Visual molecular dynamics (VMD) [32] was used for the analysis of the MD simulation trajectories as well as for the visualization and image rendering purpose. The hydrogen bonds were calculated using the hydrogen bonds plugin built in VMD taking the heavy atom distance and bond angle cut off 3.5 Å and 30°, respectively. The non-bonded interaction energies (electrostatic and van der Waals) were estimated using the NAMD energy plugin available in VMD. The solvent accessible surface area (SASA) was also calculated using VMD.

3. RESULTS AND DISCUSSION

We performed molecular dynamics simulation to assess the contribution of mCpG sites in each DNA strand in the recognition and interactions of Kaiso with meDNA sequence. We have studied Kaiso in complex with two hemimethylated DNA sequences, having different methylation states in each strand of DNA, as explained in Materials and Methods section. Fig. 1a shows the DNA nucleotide sequences in the MeECad sequence with two consecutive symmetrically methylated CpG sites at the core recognition site of Kaiso. The Kaiso-DNA complex having the methylation of the cytosine in the coding strand (5mC8 and 5mC10) as shown in fig. 1b is referred to as the hemi_C complex hereafter. By convention, the coding strand is the one that runs from 5' to 3' direction. Similarly, another complex having the methylation of the cytosine in the non-coding strand (5mC26 and 5mC28), as shown in fig. 1c, is referred to as the hemi_NC complex hereafter.

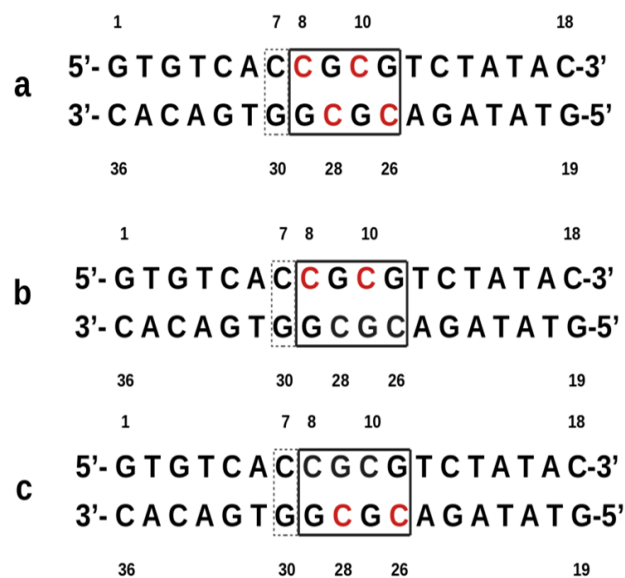


Fig. 1: Sequences of DNA nucleotides in (a) MeECad sequence, (b) hemi_C sequence having the methylated cytosines (5mC8 & 5mC10) in the coding strand (5' to 3') of DNA, (c) hemi_NC sequence having the methylated cytosines (5mC26 & 5mC28) in the non-coding strand (3' to 5') of DNA. The central boxes (with solid lines) enclose the core recognition sites. Similarly, the 5'-flanking base pairs are enclosed in dotted box. The red Cs in the central boxes correspond to the methylated cytosine bases.

3.1. Structural Stability of the Kaiso in Complex with Hemimethylated DNA

To assess the structural stability of the complexes, we calculated the root mean square deviation (RMSD) of the Kaiso-DNA complexes taking initial structure as the reference. RMSD of a molecular complex gives the idea of the conformational change in the complex during the MD simulation as compared to the initial structure. As revealed in RMSD plot in fig. 2 (a), after initial reorganization, both complexes are relatively stable after 40 ns. The hemi_NC complex shows greater value of RMSD as compared to hemi_C complex indicating relatively larger structural change of the complex. We calculated other average properties of the system on the relatively stable region of the RMSD plot, after 40 ns of the MD simulation run.

To estimate the flexibility of the individual Kaiso residues in each Kaiso-DNA complexes, we calculated the root mean square fluctuations (RMSF) of the amino acid residue in Kaiso. We calculated RMSF for the last 60 ns of the simulation trajectory after the systems were relatively stable.

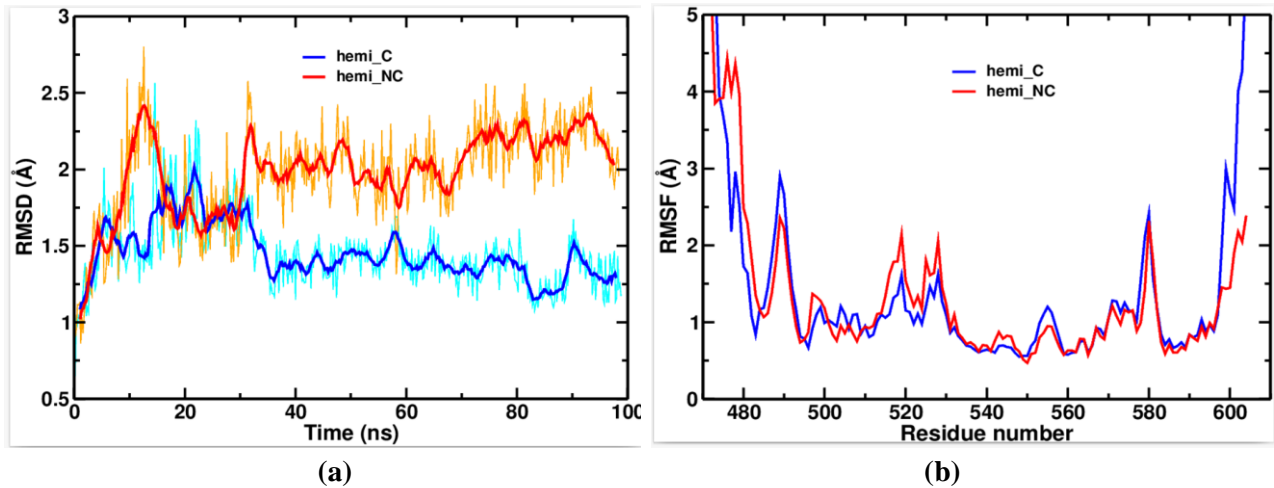


Fig. 2: (a) Time evolution of the RMSD of the Kaiso-DNA complexes and (b) RMSF measurements of Kaiso residues in hemi_C and hemi_NC complexes.

As shown in RMSF plot (fig. 2b), the fluctuation of the Kaiso residues are similar in both complexes, showing the similar stability of the Kaiso residues involved in the interactions with DNA nucleotides. The Kaiso residues in N- and C-terminal region show significantly higher value of the RMSF indicating the larger flexibility of the amino acids residues in the extremity of the proteins. The overlapping peaks in the RMSF graph are of the Kaiso residues residing in the loop joining the β -sheets of the ZF motif, which are highly flexible and are not specifically involved in the interaction with DNA. The residues with smaller value of RMSF correspond to the stable residues in the alpha helices of the ZF domain. They are involved in forming the non-covalent interactions, especially hydrogen bonds, with the DNA nucleotides.

3.2 Non-bonded Interactions between Kaiso and DNA Sequences

To investigate the difference in the binding preference of Kaiso to different hemimethylated DNA sequence, we compared the hydrogen bonding interactions between the Kaiso residues

and DNA nucleotides in both hemi_C and hemi_NC complexes. Hydrogen bonds are the major non-covalent interactions responsible for the formation of bio-molecular complexes. The number and strength of the hydrogen bonds determines the binding strength of the protein-DNA complex.

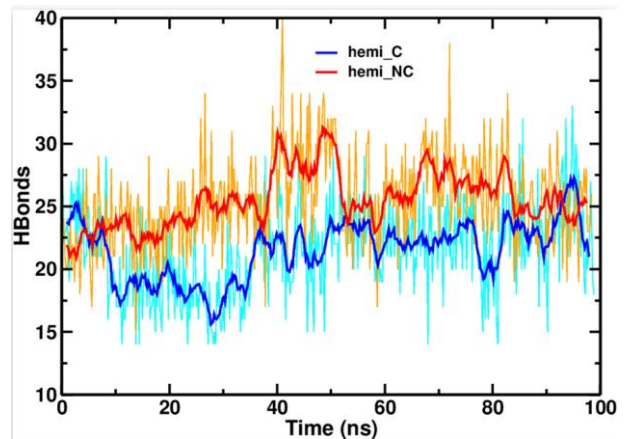


Fig. 3: Time evolution of number of hydrogen bonds formed between Kaiso residues and DNA nucleotides in the hemi_C and hemi_NC complexes.

Table 1: Occupancy percentage (> 50 %) of the hydrogen bonds formed between Kaiso residues and DNA nucleotides in both hemi_NC and hemi_C complexes.

hemi_NC complex			hemi_C complex		
Donor	Acceptor	Occupancy	Donor	Acceptor	Occupancy
ARG549-Side	5MC28-Side	196.68%	ARG549-Side	CYT28-Side	196.40%
ARG511-Side	GUA9-Side	129.16%	ARG511-Side	GUA9-Side	143.82%

CYT8-Side	GLU535-Side	104.86%	CYT28-Side	GLU535-Side	132.13%
TYR550-Side	GUA29-Side	101.02%	TYR550-Side	GUA29-Side	98.20%
THR538-Side	GUA27-Side	100.26%	TYR584-Side	GUA29-Side	96.63%
TYR584-Side	GUA29-Side	98.21%	TYR503-Side	5MC8-Side	92.58%
TYR562-Side	GUA30-Side	93.35%	THR538-Side	GUA27-Side	91.01%
TYR503-Side	CYT8-Side	90.28%	SER508-Side	GUA9-Side	90.11%
SER508-Side	GUA9-Side	87.21%	TYR562-Side	GUA30-Side	89.89%
ARG501-Side	CYT8-Side	79.28%	ARG510-Side	GUA24-Side	83.82%
VAL504-Main	GUA9-Side	77.24%	TYR536-Side	CYT7-Side	73.03%
GLY579-Main	GUA30-Side	72.12%	VAL504-Main	GUA9-Side	70.34%
GLN596-Side	5MC28-Side	71.61%	ARG501-Side	5MC8-Side	60.67%
TYR536-Side	CYT7-Side	70.59%	ARG595-Side	THY14-Side	57.08%
TYR522-Side	5MC26-Side	68.80%			
ARG603-Side	ADE21-Side	68.03%			
5MC28-Side	GLU535-Side	64.19%			
CYT5-Side	GLN563-Side	63.43%			
GLN596-Main	THY14-Side	62.15%			
TYR599-Main	THY14-Side	61.13%			
5MC26-Side	THR507-Side	55.50%			
ARG595-Side	CYT13-Side	53.71%			
LEU600-Main	THY14-Side	50.64%			

Fig. 3 shows the time evolution of the number of hydrogen bonds in two complexes for 100 ns of simulation time. The total number of hydrogen bonds in hemi_NC complex is relatively higher than that of hemi_C complex indicating the stronger binding in hemi_NC complex. We have also calculated the occupancy percentage of the major hydrogen bonds formed between the Kaiso residues and DNA nucleotides in both complexes as shown in table 1. The hydrogen bonds with occupancy percentage greater than 50 % are

greater in hemi_NC complex than in hemi_C complex, implicating the stronger binding of Kaiso with DNA in hemi_NC complex. Fig. 4a and 4b show the hydrogen bonds formed between the Kaiso residues in ZF1 and ZF2 with DNA nucleotides in core site respectively. In addition to these two domains, the residues in the ZF3 and the C-terminal extension loops are also involved in forming non-base-specific hydrogen bonds with DNA nucleotides.

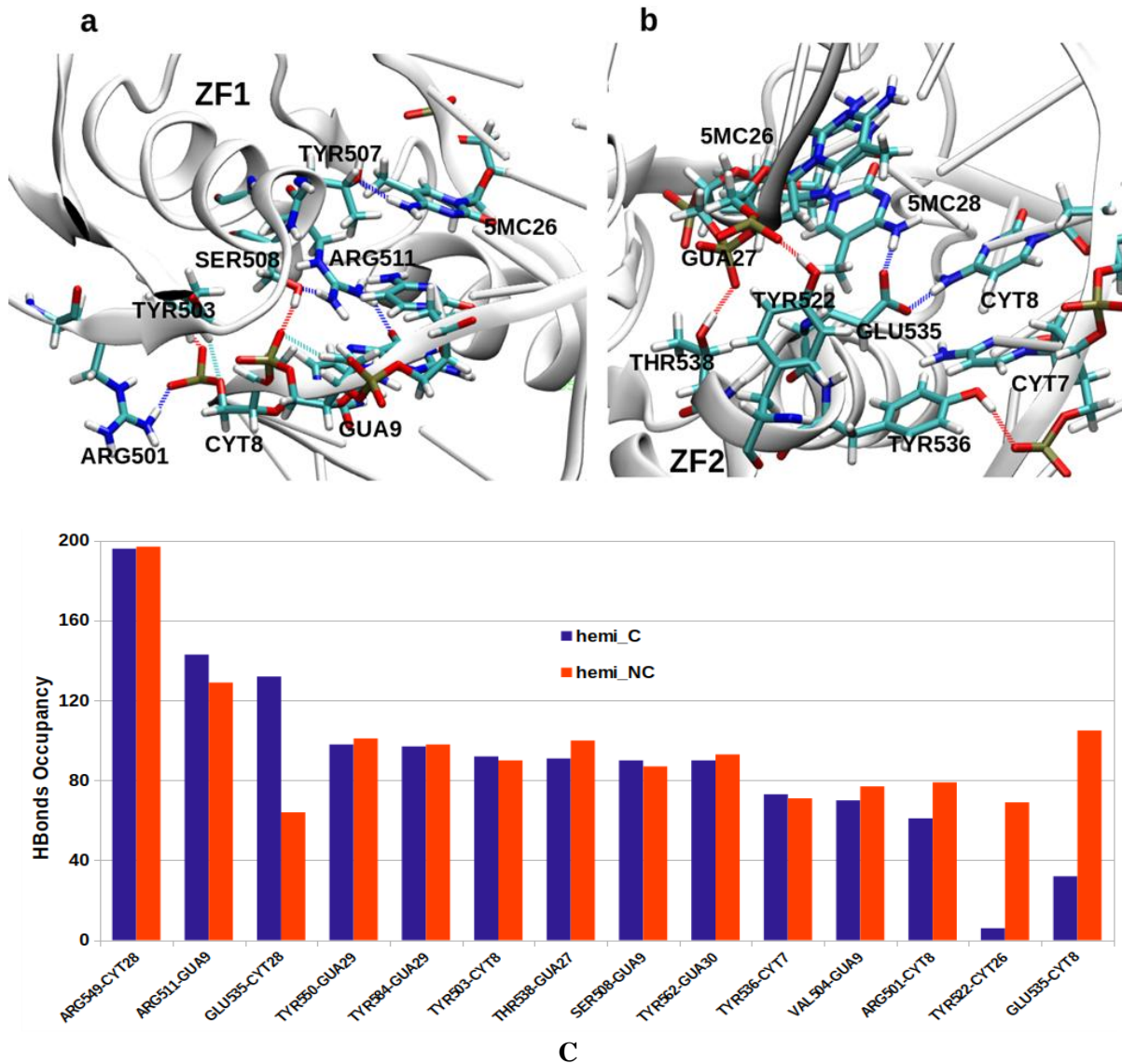


Fig. 4: Representative snapshots of the MD simulation trajectories showing the major hydrogen bonds formed by the residues in the (a) ZF1 domain of Kaiso and b) ZF2 domain of Kaiso with DNA nucleotides. c) Occupancy percentage of the major hydrogen bonds formed between the Kaiso residues and the DNA nucleotides in the core CpG sites in two complexes. In (c) The CYT8 and CYT10 in hemi_C complex and CYT26, and CYT28 in hemi_NC complex should be read as methylated cytosines (5mC).

The major hydrogen bonds formed in the core CpG recognition site are shown in fig 4c, which shows that majority of the hydrogen bonds in the core region are of similar in both complexes except for few stronger bonds in hemi_NC complex. We also studied the hydrogen bonds formed by the cytosines affected by the methylation in the core sites with the Kaiso residues. As shown in the interaction matrix in fig. 5a, the number of hydrogen bonds formed by the core cytosines are higher in hemi_NC complex. Interestingly, our results show that the base-specific hydrogen bonds formed between

GLU535 in Kaiso and CYT8 and CYT28 in DNA is higher in case of non-methylated cytosines as shown in fig 4c. The GLU535-CYT8 bond is significantly higher in hemi_NC complex than in hemi_C complex. Similarly, two additional hydrogen bonds are formed by 5mC26 with TYR522 and THR507 in hemi_NC complex (as shown in fig. 5a), whereas, these bonds are missing in hemi_C complex. Clearly, the hydrogen bonding interactions of Kaiso residues with DNA nucleotides are stronger in hemi_NC complex suggesting the higher binding affinity of Kaiso to this DNA sequence.

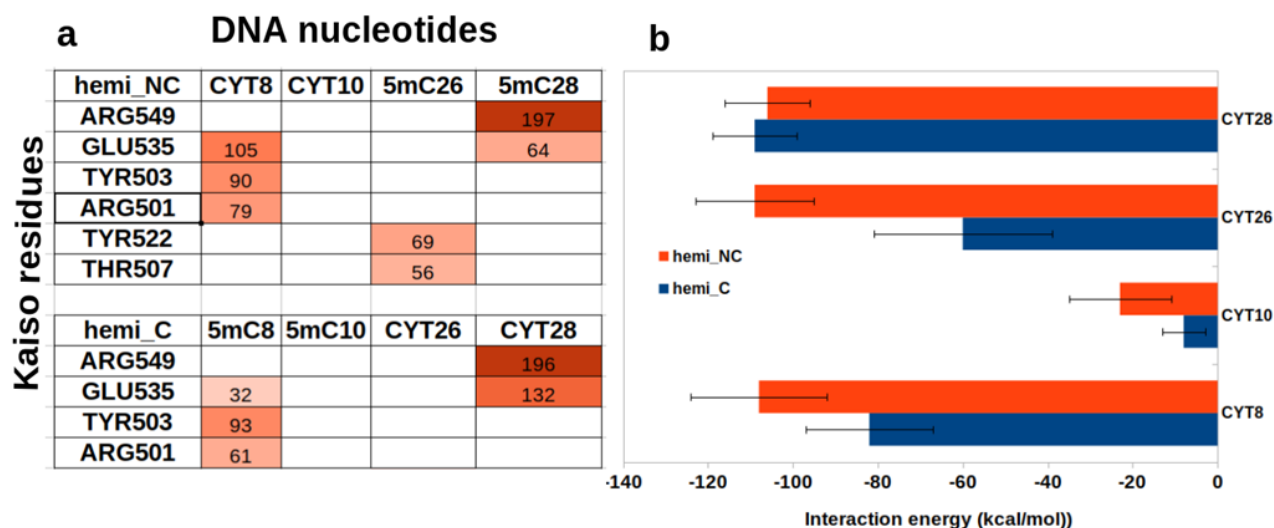


Fig. 5: a) Occupancy percentage of hydrogen bonds formed by the cytosines with Kaiso residues in the core CpG sites and b) Total non-bonded interaction energy contribution of each cytosine in the hemi_NC and hemi_C complexes.

To assess the contribution of each methylated cytosines in binding of Kaiso with DNA, we estimated the total non-bonded interaction energy of each cytosine in both hemi_C and hemi_NC complexes. As shown in fig 5b, the total interaction energy of cytosines is greater in hemi_NC complex, which implies the stronger binding in this complex.

Furthermore, we calculated the non-bonded interaction energies of total system in both complexes. As shown in table 2, both the electrostatic and van der Waals (vdW) interaction energies (average \pm std. dev) are higher in case of hemi_NC complex, showing preference of Kaiso for this DNA sequence.

Table 2: Comparison of non-bonded interactions in both hemi_C and hemi_NC complexes.

Kaiso-DNA complex	Interaction energy (kcal/mol)	
	Electrostatic	van der Waals
hemi_C	-1338.97 ± 192.87	-106.76 ± 46.87
hemi_NC	-1489.79 ± 147.18	-149.63 ± 26.23

To estimate the stability and binding strength of Kaiso to hemimethylated DNA sequences, we calculated the contact area between protein and DNA from the MD simulation trajectories. The contact area is the surface buried at the binding

interface of the Kaiso protein and DNA. For this, we first calculated the solvent accessible surface area (SASA) of the Kaiso and DNA molecules and the complex separately.

Table 3: Comparison of contact area at the binding interface of the Kaiso-DNA complex and cytosine bases with Kaiso in both hemi_C and hemi_NC complexes.

Molecular structure	Contact area (\AA^2)	
	hemi_C (5mC8 & 5mC10)	hemi_NC (5mC26 & 5mC28)
Kaiso_DNA complex	1653.39 ± 146.67	1805.14 ± 142.99
CYT8-Kaiso	188.55 ± 25.73	159.04 ± 11.11

CYT10-Kaiso	95.52±14.58	99.96±16.77
CYT26-Kaiso	161.98±19.00	211.51±15.41
CYT28-Kaiso	171.83±11.92	166.11±9.84

The contact area at the binding interface of the Kaiso-DNA complex is calculated using the following relation,

$$\sigma = \frac{S(\text{Kaiso}) + S(\text{DNA}) - S(\text{Kaiso-DNA})}{2} \dots\dots\dots (1)$$

Where, $S(\text{Kaiso})$, $S(\text{DNA})$ and $S(\text{Kaiso-DNA})$ denote the SASA of the Kaiso, DNA and Kaiso-DNA complex respectively. As revealed by the table 3, the contact area (average \pm std. dev) of the hemi_NC complex is larger than that of hemi_C complex, indicating the stronger binding in the hemi_NC complex. For this, the major contribution comes from the 5mC26, whose contact area increases upon methylation (table 3) in the hemi_NC complex.

Moreover, we estimated the binding free energy of both Kaiso-DNA complex using MM/GBSA approach. MM/GBSA binding free energy gives us efficient way to compare the binding affinity of the bio-molecular complexes. The MM/GBSA binding free energy of the hemi_NC complex is found to be -124.56 ± 3.14 kcal/mol and that of hemi_C is found to be -90.68 ± 3.66 kcal/mol. Therefore, the binding affinity of Kaiso is clearly higher for the sequence having methylation in non-coding strand of DNA.

4. CONCLUSIONS

In this work, we performed molecular dynamics simulations to investigate the recognition and binding of Kaiso with DNA sequences having different methylated states of core CpG sites. To assess the contribution of methylation in each strand, we studied the interactions of Kaiso with two different hemimethylated DNA sequences; methylated CpG sites in coding (hemi_C complex) and non-coding (hemi_NC complex) strand of DNA. Our results show that binding of Kaiso with DNA sequence having the methylation in the non-coding strand (5mC26 and 5mC28) is stronger than the methylation in the coding strand (5mC8 and 5mC10). The total number of hydrogen bonds in case of hemi_NC complex are greater than that in hemi_C complex. The major hydrogen bonds

formed in the core CpG site in both complexes are similar; however, few bonds are stronger in hemi_NC complex. The ARG511 in ZF1 and GLU535 in ZF2 are involved in the base-specific hydrogen bonding interactions with DNA bases in both sequences. We found that the GLU535 forms hydrogen bond with CYT8 and CYT28 in core CpG site in both sequences. Interestingly, our results show the stronger hydrogen bonds are formed between GLU535 with unmethylated cytosines (CYT8 and CYT28) than that with methylated ones (5mC8 and 5mC28). Similarly, the residues in ZF3 and C-terminal extension loop are involved in the interaction with the backbone phosphate group to anchor the ZF domains to the DNA. Similarly, the non-bonded interactions energies, both electrostatic and van der Waals are also higher in hemi_NC complex. In addition, the contact area at the Kaiso-DNA binding interface is greater in hemi_NC complex. Moreover, the MM/GBSA binding free energy is also higher for the binding of Kaiso with the DNA having methylation in non-coding strand. To sum up, even though Kaiso binds with significant affinity to both hemimethylated DNA sequences, it prefers the methylated CpG sites in the non-coding strand. Methylation on the non-coding strand (5mC26 and 5mC28) of DNA plays important role in the binding of Kaiso with methylated DNA sequence.

ACKNOWLEDGEMENTS

BT and NPA acknowledge the TWAS research grant RG 20-316. BT also acknowledges the PhD Fellowship and Research Support Grant (Award number PhD-78/79-S&T-15) from the University Grants Commission (UGC), Nepal.

REFERENCES

- [1] Klose, R. J. and Bird, A. P. Genomic DNA methylation: the mark and its mediators. *Trends Biochem. Sci.*, **31**: 89-97 (2006).
- [2] Bird, A. The essentials of DNA methylation. *Cell*, **70**: 5-8 (1992).
- [3] Bird, A. DNA methylation patterns and epigenetic memory. *Genes Dev.*, **16**: 6-21 (2002).

- [4] Miranda, T. B.; and Jones, P. A. DNA methylation: the nuts and bolts of repression. *J. Cell. Physiol.*, **213**: 384-390 (2007).
- [5] Blasi, F.; and Toniolo, D. DNA methylation and X-chromosome inactivation. *Mol. Biol. Med.*, **1**: 271-274 (1983).
- [6] Li, E.; Beard, C.; and Jaenisch, R. Role for DNA methylation in genomic imprinting. *Nature*, **366**: 362-365 (1983).
- [7] Jones, P. A.; and Takai, D. The role of DNA methylation in mammalian epigenetics. *Science*, **293**: 1068-1070 (2001).
- [8] Robertson, K. D. DNA methylation and human disease. *Nat. Rev. Genet.*, **6**: 597-610 (2005).
- [9] Rottach, A.; Leonhardt, H.; and Spada, F. DNA methylation-mediated epigenetic control. *J. Cell. Biochem.*, **108**: 43-51 (2009).
- [10] Clouaire, T.; and Stancheva, I. Methyl-CpG binding proteins: specialized transcriptional repressors or structural components of chromatin? *Cell. Mol. Life Sci.*, **65**: 1509-1522 (2008).
- [11] Wade, P. A. Methyl CpG-binding proteins and transcriptional repression. *Bioessays*, **23**: 1131-1137 (2001).
- [12] Yoon, H.-G.; Chan, D. W.; Reynolds, A. B.; Qin, J.; and Wong, J. N-CoR mediates DNA methylation-dependent repression through a methyl CpG binding protein Kaiso. *Mol. Cell*, **12**: 723-734 (2003).
- [13] Hendrich, B.; Bird, A. Identification and characterization of a family of mammalian methyl CpG-binding proteins. *Genetics Res*, **72**: 59-72 (1998).
- [14] Bostick, M.; Kim, J. K.; Estève, P.-O.; Clark, A.; Pradhan, S.; and Jacobsen, S. E. UHRF1 plays a role in maintaining DNA methylation in mammalian cells. *Science*, **317**: 1760-1764 (2007).
- [15] Fillion, G. J. P.; Zhenilo, S.; Salozhin, S.; Yamada, D.; Prokhortchouk, E.; Defossez, P.-A. A family of human zinc finger proteins that bind methylated DNA and repress transcription. *Mol. Cell. Biol.*, **26**: 169-181 (2006).
- [16] Sasai, N.; Nakao, M.; and Defossez, P.-A. Sequence-specific recognition of methylated DNA by human zinc-finger proteins. *Nucleic Acids Res.*, **38**: 5015-5022 (2010).
- [17] Liu, Y.; Zhang, X.; Blumenthal, R. M.; and Cheng, X. A common mode of recognition for methylated CpG. *Trends Biochem. Sci.*, **38**: 177-183 (2013).
- [18] Daniel, J. M.; and Reynolds, A. B. The catenin p120 ctn interacts with Kaiso, a novel BTB/POZ domain zinc finger transcription factor. *Mol. Cell. Biol.*, **19**: 3614-3623 (1999).
- [19] Prokhortchouk, A.; Hendrich, B.; Jørgensen, H.; Ruzov, A.; Wilm, M.; Georgiev, G.; Bird, A. and Prokhortchouk, E., The p120 catenin partner Kaiso is a DNA methylation-dependent transcriptional repressor. *Genes Dev.*, **15**: 1613-1618 (2001).
- [20] Daniel, J. M.; Spring, C. M.; Crawford, H. C.; Reynolds, A. B.; and Baig, A. The p120 ctn-binding partner Kaiso is a bi-modal DNA-binding protein that recognizes both a sequence-specific consensus and methylated CpG dinucleotides. *Nucleic acids res.*, **30**: 2911-2919 (2002).
- [21] Blattler, A.; Yao, L.; Wang, Y.; Ye, Z.; Jin, V. X.; and Farnham, P. J. ZBTB33 binds unmethylated regions of the genome associated with actively expressed genes. *Epigenetics Chromatin*, **6**: 1-18 (2013).
- [22] Lopes, E. C.; Valls, E.; Figueroa, M. E.; Mazur, A.; Meng, F.-G.; Chiosis, G.; Laird, P. W.; Schreiber-Agus, N.; Grealley, J. M.; and Prokhortchouk, E. Kaiso contributes to DNA methylation-dependent silencing of tumor suppressor genes in colon cancer cell lines. *Cancer Res.*, **68**: 7258-7263 (2008).
- [23] Basseby-Archibong, B. I.; Rayner, L. G. A.; Hercules, S. M.; and Aarts, C. W.; Dvorkin-Gheva, A.; Bramson, J. L.; Hassell, J. A. and Daniel, J. M. Kaiso depletion attenuates the growth and survival of triple negative breast cancer cells. *Cell Death Dis.*, **8**: e2689 (2017).
- [24] Wang, H.; Liu, W.; Black, S.; Turner, O.; Daniel, J. M.; Dean-Colomb, W.; He, Q. P.; Davis, M.; and Yates, C. Kaiso, a transcriptional repressor, promotes cell migration and invasion of prostate cancer cells through regulation of miR-31 expression. *Oncotarget*, **7**: 5677 (2016).
- [25] Buck-Koehntop, B. A.; Stanfield, R. L.; Ekiert, D. C.; Martinez-Yamout, M. A.; Dyson, H. J.; Wilson, I. A.; and Wright, P. E. Molecular basis for recognition of methylated and specific DNA sequences by the zinc finger protein Kaiso. *Proc. Natl. Acad. Sci. U.S.A.*, **109**: 15229-15234 (2012).
- [26] Nikolova, E. N.; Stanfield, R. L.; Dyson, H. J.; and Wright, P. E. CH... O hydrogen bonds mediate highly specific recognition of methylated CpG sites by the zinc finger protein Kaiso. *Biochem.*, **57**: 2109-2120 (2018).
- [27] Thapa, B., Adhikari, N. P., Tiwari, P. B., and Chapagain, P. P. A 5'-flanking C/G pair at the core region enhances the recognition and binding of Kaiso to methylated DNA. *J. Chem. Inf. Model.*, **63**(7): 2095-2103 (2023).
- [28] Lee, J.; Cheng, X.; Swails, J. M.; Yeom, M. S.; Eastman, P. K.; Lemkul, J. A.; Wei, S.; Buckner, J.; Jeong, J. C.; Qi, Y.; Jo, S.; Pande, V. S.; Case, D. A.; Brooks, C. L., 3rd; MacKerell, A. D., Jr.; Klauda, J. B.; and Im, W. CHARMM-GUI Input Generator for NAMD, GROMACS,

- AMBER, OpenMM, and CHARMM/OpenMM Simulations Using the CHARMM36 Additive Force Field. *J. Chem. Theory Comput.*, **12** (1): 405-13 (2016).
- [29] Phillips, J. C.; Braun, R.; Wang, W.; Gumbart, J.; Tajkhorshid, E.; Villa, E.; Chipot, C.; Skeel, R. D.; Kale, L.; and Schulten, K. Scalable molecular dynamics with NAMD. *J. Comput. Chem.*, **26**: 1781-1802 (2005).
- [30] Huang, J.; and MacKerell Jr, A. D., CHARMM36 all-atom additive protein force field: Validation based on comparison to NMR data. *J. Comput. Chem.*, **34**: 2135-2145 (2013).
- [31] Essmann, U.; Perera, L.; Berkowitz, M. L.; Darden, T.; Lee, H.; and Pedersen, L. G. A smooth particle mesh Ewald method. *J. Chem. Phys.*, **103**: 8577-8593 (1995).
- [32] Humphrey, W.; Dalke, A.; and Schulten, K., VMD: visual molecular dynamics. *J. Mol. Graph.*, **14**: 33-38 (1996).